Assessing Shoreline Dynamics of Manpura Island (Meghna Estuary in Bangladesh) from 2000 to 2024 Using Remote Sensing and DSAS Techniques

Hridoy Saha[1], Iftakhar Ahmed[2], Mahfujur Rahman[3], Anika Samm-A[2*] and Mahmudul Hasan[1]

[1]Department of Oceanography, University of Dhaka, Dhaka 1000, Bangladesh
[2]Department of Disaster Science and Climate Resilience, University of Dhaka, Dhaka 1000, Bangladesh
[3]Department of Geology, University of Dhaka, Dhaka 1000, Bangladesh

Manuscript received: 23 April 2025; accepted for publication: 30 November 2025

ABSTRACT: Coastal areas in Bangladesh are highly susceptible to climate change due to their geographical location and geological characteristics. To better understand the vulnerability and the dynamic nature of coastal changes, this study focuses on Manpura Island (an offshore island located at the confluence of the Meghna River and the Bay of Bengal), where the impacts of climate change and coastal processes are particularly pronounced. To assess this shoreline dynamic changes, first the island was delineated and analyzed between 2000 and 2024 utilizing GIS and automated computations with DSAS techniques. This study has been broadly assessed based on the Transect-based shoreline change using End Point Rate (EPR), Weighted Linear Regression (WLR), and Linear Regression Rate (LRR). Regarding the erosion and accretion of the island, the result shows that the highest erosion rate recorded was 227.2 m/year, where the peak accretion rate was about 14.5 m/year. The study revealed a net land loss of 26.26 km², with an average annual loss of 1.09 km². Besides, the greatest amount of erosion (10.95 km²) emerged in between 2005 and 2010, and between 2010 and 2015 it accounted as 10.15 km². To support our satellite based investigation, a comprehensive survey was conducted at the field level to validate the findings of the study. A precise assessment of this offshore islands' vulnerability is crucial as Bangladesh coastal areas is frequently affected by the natural disasters. The findings of the study may enable the legislatures, local government, and environmental conservators to take effective coastal management strategies to mitigate further land loss of the island.

Keywords: Coastal Erosion; Shoreline Change; Geospatial Analysis; Manpura Island; Meghna Estuary

INTRODUCTION

Globally, coastal regions are the most vulnerable areas to climate change induced extreme natural hazards. Coastal erosion is one of these phenomena that influence not only the socio-economic dynamics of inhabitants but also the ecological balance of any particular region. Erosional activities at the coast occur as a result of combination of multiple settings, particularly meteorology, morphology, and geology in the given locality. Climate change, extreme weather events, natural processes (extreme waves, tropical storms, sedimentary imbalance, etc.) are considered primary contributors to the erosion in the coastal region. Additionally, anthropogenic factors (such as unregulated deforestation, alterations in land use, unplanned urbanization, rapid industrialization, imprecise planning of dams and embankments, illegal infrastructure establishment, sand mining, etc.) enhance the erosion process and affect the shoreline and coastline. (Coca and Ricaurte-Villota, 2022; Duvat, 2019; Kumar et al., 2018; Thomas and Benjamin, 2018; Vallarino-Castillo et al., 2024).

Coastline erosion and accretion are prominent issues affecting different regions globally. Islands of Pacific and Caribbean have been reported to experience both coastal and riverbank erosion. Similarly in India, the regions of Assam, Tripura, and West Bengal have been consistently identified as being highly vulnerable to riverbank erosion (Ahmed et al., 2018; Bhowmik et al., 2018; Chatterjee and Mistri, 2013; Debanshi and Mandal, 2014; Dutta et al., 2010; Khan, 2012), while the coastal areas of Tamil Nadu, Gujarat, Vishakhapatnam, and Karnataka are struggling with ongoing coastal erosion (Chirala et al., 2015; Gorle et al., 2024; Kannan et al., 2016; Pereira et al., 2022; Ramalho et al., 2013). A study in Yilan County, Taiwan, revealed that the coast accretes in the summer due to sediment influx

Corresponding author: Anika Samm-A
E-mail: anikasamma@du.ac.bd

DOI: https://doi.org/10.3329/dujees.v14i2.87595

from rivers, while in winter, erosion occurs because of waves from the northeast monsoon (Liang et al., 2022). Changes on the Red Sea coast of Saudi Arabia between Al Lith and Ras Mahasi displayed considerable erosion, notably in the southern region, driven by wave action and storms, while minor accretion occurred in the north (Al-Zubieri et al., 2020).

To monitor coastal morphology dynamics, several techniques have been developed, including direct distance measurements, laser scanning, camera-based monitoring, and aerial photography (Mentaschi et al., 2018). These methods have significantly improved the understanding of coastal pattern changes at both local and regional scales. Considering the cost and manpower constraints, remote sensing and GIS are regarded as convenient and cost-effective tool. Among the various techniques available for shoreline dynamics assessment, the Digital Shoreline Analysis System (DSAS) provides a standardized and statistically robust framework for quantifying coastal change through time. Unlike other approaches that focus solely on shoreline delineation, DSAS integrates multi-temporal shoreline datasets and computes several quantitative metrics such as the End Point Rate (EPR), Simple Linear Regression (SLR), Weighted Linear Regression (WLR), and least median of squares (Thieler et al., 2009). These metrics allow for accurate estimation of long-term trends, while also providing uncertainty and confidence intervals, thereby improving the reliability of change detection (Himmelstoss et al., 2018). Therefore, DSAS technique is found to be a significant method to enumerate the shoreline dynamics. Globally, in many regions such as the north Sinai coast of Egypt, the northwest coast of Mauritius, Quang Nam Province of Vietnam, etc., the DSAS method was used to evaluate coastal and shoreline dynamics (Nassar et al., 2019; Bheeroo et al., 2016; Quang et. al., 2021)

Bangladesh, a riverine country historically suffers from both riverbank and coastal erosion, similar to its neighboring countries. Specifically, the braided river chars and the coastal islands are frequently reported to suffer from erosional activities (Ahmed et al., 2020, 2021; Haque et al., 2023; Islam et al., 2023; Khan and Islam, 2003; Rahman, 2010; Saha et al., 2022). Among these, the erosion of the islands should be addressed with more concern because they are particularly vulnerable to sea level rise, tidal wave action, and annual cyclonic events with storm surge and inundation. When erosion particularly occurs on any island, it becomes extremely difficult to relocate people who have lost their homesteads and livelihood-related lands due to limited space. In certain regions, industries reliant on coastal fisheries experience disruption, leading to financial losses (Ahmed et al., 2021; Bernzen et al., 2019; Islam et al., 2021, 2019). Furthermore, the aesthetic and ecological degradation resulting from coastal erosion may adversely impact tourism activities on certain islands (Dukes and Mooney, 2004; Pimentel and Kounang, 1998).

Amongst these coastal islands, Manpura Island of Bangladesh is the main focus of this study which faces annual land loss event due to erosion. The study particularly chose this island for the investigation of erosional study because the area is situated at the confluence of river Meghna and Bay of Bengal. Riverine and coastal dynamics are playing significant roles in the erosional process in the island. Residents over the island are experiencing severe shrinking of their homestead and agricultural land, followed by affected livelihood and socio-economic condition. Multiple respondents are reported to be the victim of repeated land loss even after shifting from their previous place (Ali et al., 2013; Biswas et al., 2022; The Daily Star, 2017). Apart from these, frequent erosion is affecting the island's significant potential to be designed as an eco-tourism sector.

In these regard, this study incorporated the Digital Shoreline Analysis System (DSAS) to understand the dynamic shoreline changes of this island from 2000 to 2024. By leveraging DSAS within ArcGIS, this study provides a more accurate, automated, and efficient approach to analyzing shoreline changes over the specified time frame. The primary aim is to update and refine previous analyses by extending the study period from 2000 to 2024, ensuring a comprehensive understanding of shoreline dynamics is utmost in this regard. Therefore, this research seeks to generate reliable data for better coastal management, policy-making, and mitigation strategies by assessing the combined influence of climate change and human activities on shoreline retreat, ultimately supporting sustainable coastal resilience efforts and directly advancing different SDGs (SDG 13- Climate Action, SDG11- Sustainable Cities, SDG 1-No Poverty). (United Nations, 2015)

MATERIALS AND METHODS

Study Area

The area selected for this research is Manpura Island, which is located near the mouth of the Meghna River in the northern Bay of Bengal. Its geographic coordinates are as follows: latitudes about 22°02.63′N to 22°20.85′N, longitudes 90°52.28′E to 90°98.00′E. The island is totally surrounded by ocean, and the Meghna River's expanse to the west and south forms its boundaries. Manpura Island shares borders with Hatiya Island to the east, the Shahbazpur Channel to the west, and Char Patlia and Char Nizam to the north (Fig. 1). Due to its unique location near the coastal zone of Bangladesh, it has become a somewhat interesting subject of coastal research. The area of the island is 373 km². The Manpura Island is a flat landmass; the highest peak is around three meters above sea level (Ahmed et al., 2018). There are some highlands on the island, but these are man-made, like roads and embankments (Ali et al., 2013). Manpura Island has calcareous alluvium and saline soil. Begum and Billah (2012) have studied the morphological, mineralogical, and edaphological aspects of the soil of Manpura Island and found predominately loamy soil with an average content of 51% silt and 21% clay with colors varying from very dark grey to dark grey. It is formed in relatively recent, medium-textured deposits, inadequate drainage, and floods seasonally. On the young lower Meghna estuary floodplain, it is widely distributed.

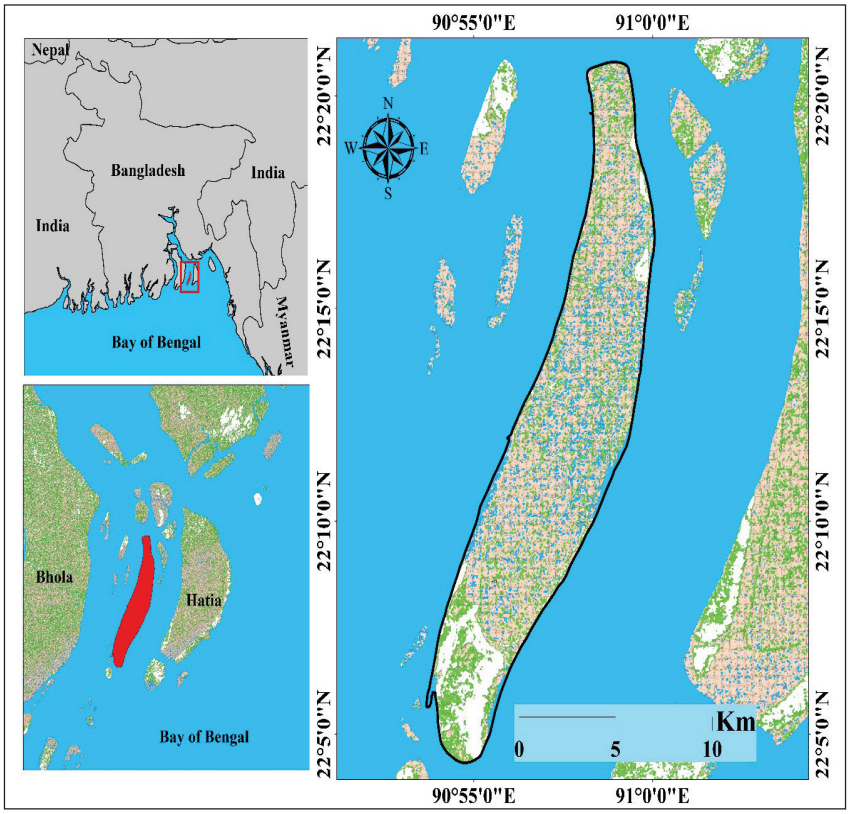

Figure 1: Location Map of the Study Area

Datasets Used

Multi-temporal Landsat satellite imageries (six scenes) from 2000-2024 time periods are considered to select based on its various satellite sensors such as Landsat TM (Thematic Mapper), ETM+ (Enhanced Thematic Mapper Plus), and OLI (Operational Land Imager). These images were taken from US Geological Survey (USGS) to monitor the shoreline's position. The details of the above-mentioned Landsat satellites sensors are given in Table 1. The cloud coverage of these images was mostly less than 5% which was applied as the set criteria during the image acquisition. Additionally, the primary time period of these images was set to January to middle of May because the images accommodate less cloud covered during this time.

Table 1: Satellite Image Information of Different Years

Satellite	Sensor Type	Path/ Row	Acquisition Date	Cloud Cover (%)	Pixel Resolution (m)	Image Acquisition Time (GMT+6)
Landsat 5	TM	136/045	01/14/2000	< 5	30	09:58
Landsat 5	TM	136/045	02/10/2005	< 5	30	10:05
Landsat 7	ETM+	136/045	03/23/2010	< 5	30	10:08
Landsat 8	OLI	136/045	02/25/2015	< 4	30	10:19
Landsat 8	OLI	136/045	02/20/2020	< 3	30	10:20
Landsat 8	OLI	136/045	01/30/2024	< 5	30	10:23

Methodology

Methodological Overview

The study opted the simplified form of DSAS workflow to measure the dynamics of the shorelines in the Manpura Island. Six Cloud-free Landsat 5-8, level-2 images were collected at a 5 years interval. Digitization of a geodetically controlled baseline and orthogonal transects were created in DSAS that upon which we measured the Shoreline Change Envelope (SCE), Net Shoreline Movement (NSM), End-Point Rate (EPR), and (Weighted) Linear Regression Rate (LRR/WLR) using user-defined positional and proxy errors. Representative shoreline positions were verified using limited field validation (ground-truth points and photographs) and then, spatial and statistical analysis was conducted to identify the significant zones of erosion and accretion and area change. Despite all the methods of erosion and accretion, such as the detection of the shoreline using optical imagery through Normalized Difference Water Index (NDWI) (McFeeters, 1996), Modified Normalized Difference Water Index MNDWI (Xu, 2006), and AWEI (Feyisa et al., 2014); the use of historical maps, aerial photography, and photogrammetry (Boak and Turner, 2005); continuous video monitoring (ARGUS) of the swash and contour positions (Holman and Stanley, 2007); DSAS (Thieler et al., 2009; Himmelstoss et al., 2018; 2021) was chosen because it best matches our resource, access, and time-series constraints. It influences freely available multi-decadal imagery, enforces a transparent baseline such as transect geometry, and produces uncertainty addressed statistical rates that are essential for the decision making of efficient yet resource constraint coastal management.

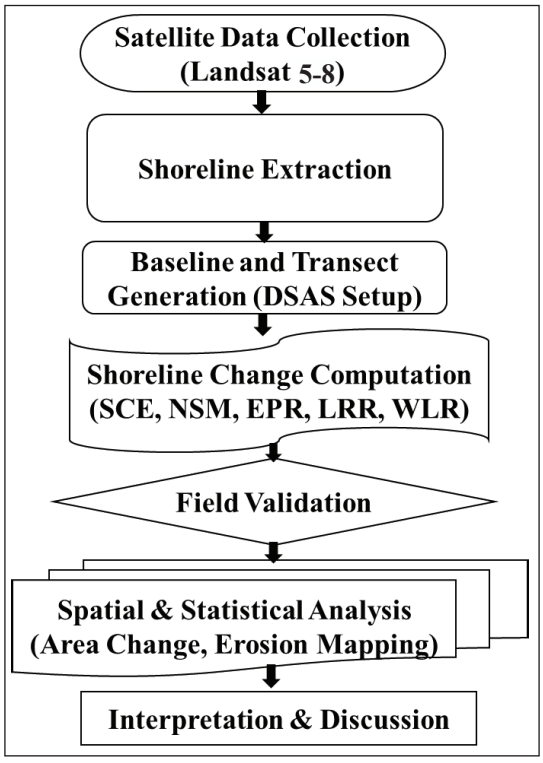

Figure 2: Methodological Framework of the Study

Image Preprocessing Method

The Landsat images used in this study were Level-2 surface reflectance products obtained from the USGS archive. These products are already geometrically and atmospherically corrected, providing surface reflectance

values derived using the Landsat Surface Reflectance Code (LaSRC) for Landsat 8 and the LEDAPS algorithm for Landsat 5–7. Therefore, no additional atmospheric correction was required prior to analysis.

The study area was defined using a boundary polygon shapefile, and a semi-automated approach was employed for shoreline extraction, which is considered as an effective method compared to fully automated methods (Dewan et al., 2017; Gupta et al., 2013; Yang et al., 1999). Shorelines were digitized as vector polylines in ArcGIS 10.5, with the water boundary representing the island's shoreline (Mahmud et al., 2020; Nicoll and Hickin, 2010). Finally, all processed images were exported to ArcGIS for shoreline digitization.

Shoreline Delineation Method

The present study employed a manual digitization approach to delineate shorelines around Manpura Island, integrating a semi-automated technique to achieve significant accuracy (Hasan et al 2022; Dewan et al., 2017; Gupta et al., 2013). The shortwave infrared (SWIR) band was utilized to distinguish the land-water interface due to its strong water absorption properties and high reflectance over land and vegetation. Specifically, shoreline visibility was enhanced using Band 5 of Landsat 5 TM, Landsat 7 ETM+ (1.55–1.75 μm), and Band 6 of Landsat 8 OLI (1.56–1.66 μm). To further refine the classification, a Normalized Difference Vegetation Index (NDVI) was applied, effectively differentiating land from water bodies (Al-Zubieri et al., 2020; Sun et al., 2012). Shoreline digitization was conducted, where water boundaries were manually traced and these were extracted at five-year intervals, generating six distinct shoreline datasets, each saved as a polyline shapefile for subsequent analysis. This method, widely adopted in shoreline studies, provides a reliable representation of coastal changes over time while mitigating inaccuracies associated with fully automated approaches (Frazier and Page, 2000; Ghorai and Mahapatra, 2020; Nassar et al., 2019).

Change Rate Calculation

The Digital Shoreline Analysis System (DSAS) Version 5.0, developed by the US Geological Survey (USGS) as an extension for Esri ArcGIS, was utilized to quantify shoreline change rates following the digitization of shoreline positions (Himmelstoss et al., 2021). This tool requires a reference baseline and at least four shoreline datasets to function effectively. A geospatial analytical framework was used to produce transects in order to facilitate a thorough evaluation of coastal dynamics surrounding Manpura Island. Transects were set up 500 meters apart and perpendicular to the shoreline to provide thorough coverage inland across a range of coastal morphologies. Along the seashore, 100-meter intervals were also kept, ensuring consistent spatial resolution for longitudinal investigation. Because of this arrangement, 743 transects were created, which served as the foundation for highly accurate shoreline change metrics calculations. These transects intersected multiple shoreline positions, serving as reference points for computing shoreline change statistics. DSAS automates the process of selecting measurement locations and calculating various shoreline change metrics, offering a standardized approach for analyzing coastal dynamics.

To assess shoreline evolution, five statistical techniques were applied, such as End Point Rate (EPR), Linear Regression Rate (LRR), Least Median of Squares (LMS), Weighted Linear Regression (WLR), and Net Shoreline Movement (NSM). EPR, LRR, and WRR express shoreline change rates in meters per year, while NSM and Shoreline Change Envelope (SCE) measured absolute displacement in meters. These methods facilitate the evaluation of historical shoreline fluctuations, aiding in the prediction of future trends, which is crucial for coastal management, hazard mitigation, and sustainable development planning.

End Point Rate (EPR)

The EPR is a method for calculating shoreline change rates. It is determined by measuring the distance between two shoreline positions at different time intervals and dividing this distance by the number of years between the two observations. The formula for EPR is given in Equation 1:

$$EPR=(L_1-L_2)/(T_1-T_2) \qquad (i)$$

Where, L_1 and L_2 represent the shoreline positions at two different time periods. T_1 and T_2 denote the corresponding years of shoreline observation. EPR provides a straightforward estimate of shoreline movement, making it a popular method in coastal

research. However, since it only considers two shoreline positions, it does not account for variations in shoreline movement trends over time, which may lead to uncertainties when assessing long-term shoreline changes.

Linear Regression Rate (LRR)

The LRR is a statistically robust method that calculates shoreline change rates by fitting a least squares regression line to multiple shoreline positions along a transect. This method helps reduce the impact of outliers and provides a more reliable estimate of long-term shoreline movement. The LRR equation is expressed as:

$$L = b + mx \qquad \text{(ii)}$$

where, L represents the shoreline position (in meters) relative to a fixed baseline, x denotes the time interval (years), m is the slope of the regression line (shoreline change rate in meters per year), and b is the y-intercept.

Least Median of Squares (LMS)

The LMS method is another regression-based approach for estimating shoreline change rates. Unlike LRR, which minimizes the sum of squared residuals, LMS minimizes the median of squared residuals, making it more resistant to outliers. This technique is particularly useful in cases where shoreline positions are affected by extreme variations due to storms, human interventions, or seasonal fluctuations.

Net Shoreline Movement (NSM) and Weighted Linear Regression (WLR)

The Net Shoreline Movement (NSM) method calculates the total shoreline displacement over a specific period. Unlike EPR, which provides a rate of change per year, NSM simply measures the absolute distance the shoreline has moved between two time periods. This is particularly useful for understanding cumulative shoreline changes over longer timescales.

The WLR refines the linear regression approach by assigning weights to the data points, minimizing the sum of squared residuals. The best-fit line is drawn such that it intersects the points in a manner that reflects the weighting, ensuring a more accurate representation of shoreline movement trends. To ensure statistical reliability, the coefficient of determination (R^2) is used to evaluate the accuracy of the regression model. To justify DSAS outputs, historical shoreline positioning was visually analyzed. In connection to this, a landward movement of the shoreline was interpreted as erosion, denoted by a negative sign, and a seaward movement as accretion, denoted by a positive sign (Anders and Byrnes, 1991).

Validation Method

To ensure the accuracy of the investigation, a comprehensive field work was conducted in this Island based on the governing parameters of the shoreline instability. In that regard, a map delineating the primary zones were produced using GIS tool. Some active zones were selected for the survey based on that zonation map and a semi-structured questionnaire was formulated to conduct the survey. Infrastructures related to housing and transportation were specifically identified by taking geographic locations into account. Individuals whose age is 40 years plus were selected for the questionnaire interview due to their experience observing the alterations in the shoreline throughout the years. After being questioned about shoreline alteration for the past 25 years, local people have recognized the areas that have changed. Finally, a contrast check of the field survey and the DSAS analyzed map was made using data collected from the in-situ questionnaire survey. The only aim of this survey was to validate the DSAS output.

RESULTS AND DISCUSSIONS

Changes in Length and Area of Shorelines from 2000 to 2024

Manpura Island, located in a dynamic deltaic region, has been significantly affected by erosion and accretion processes. In 2000, the island's shoreline measured approximately 73.22 kilometers, but by 2024, it decreased to 63.85 kilometers-a total reduction of 9.37 kilometers over 24 years (approximately at 300m/year change rate). Figure 3a illustrates the changing coastline patterns from 2000 to 2024, highlighting a consistent decline in shoreline length. The most severe erosion occurred around 2010 and 2015.

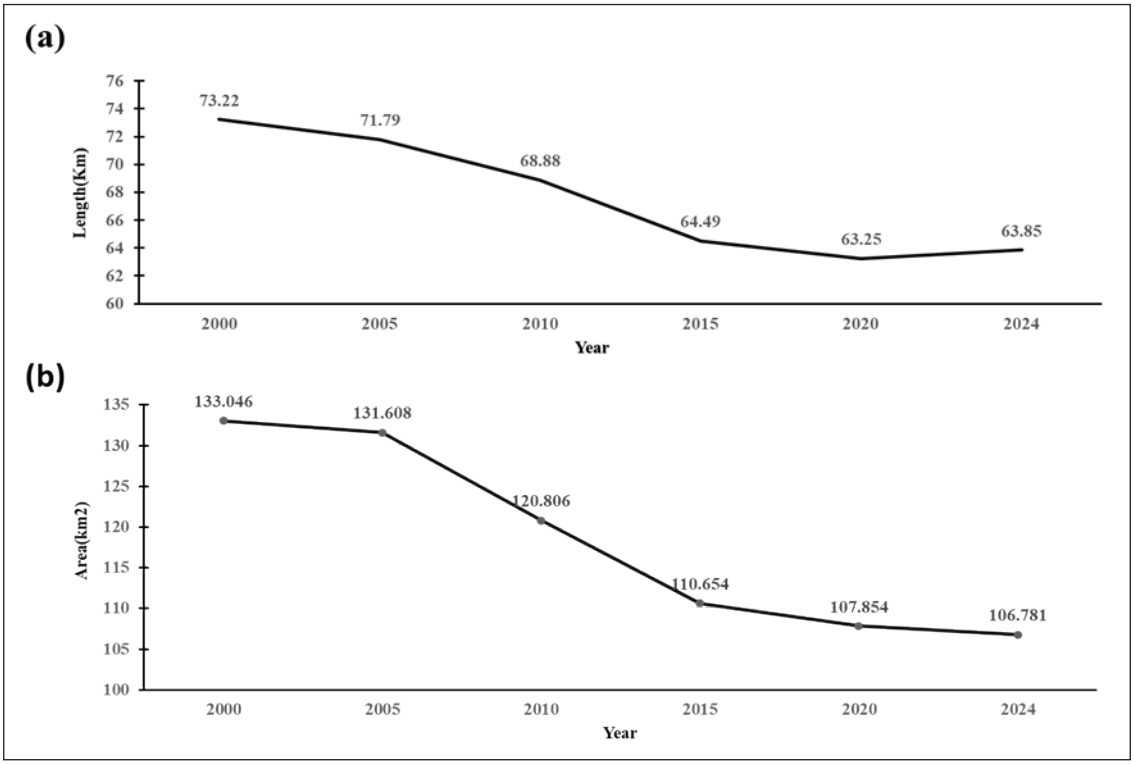

Figure 3: (a) Shoreline Length Change and (b) Area Change in Manpura Island

Analysis of the data (Fig. 3b) unveils a discernible pattern in the area change dynamics of Manpura Island. Over the span of 24 years (2000 to 2024), there is a clear downward trajectory in the island's area change trend. Between 2000 and 2024, Manpura Island lost a total of 26.265 km^{2}of land due to erosion (Table 2), averaging an annual loss of 1.093 km². The most significant erosion was recorded between 2005 and 2010, resulting in a loss of 10.952 km² (Fig. 4). Another major erosion event occurred between 2010 and 2015, leading to a further reduction of 10.156 km². In contrast, the highest land accretion was observed between 2000 and 2005, contributing only 1.877 km² to the island's area. However, this minor gain was ultimately outweighed by later erosion events, leading to a net decline in landmass. Spatial analysis indicates a dominant trend of erosion from 2000 to 2024, with no substantial long-term land gain.

Table 2: Erosion-Accretion and Area Change of Manpura Island

Year	Area (km^2)	Net loss/ gain (km^2)	Erosion (km^2)	Accretion (km$^{2)}$	Unchanged (km^2)
2000	133.046				
2005	131.608	-1.44	3.315	1.877	129.731
2010	120.806	-10.802	10.952	0.150	120.656
2015	110.654	-10.153	10.156	0.003	110.650
2020	107.854	-2.800	3.054	0.255	107.600
2024	106.781	-1.073	1.352	0.279	106.502
Period		Total	Total	Total	
24 years		-26.265 km^2	28.829 km^2	2.564 km^2	

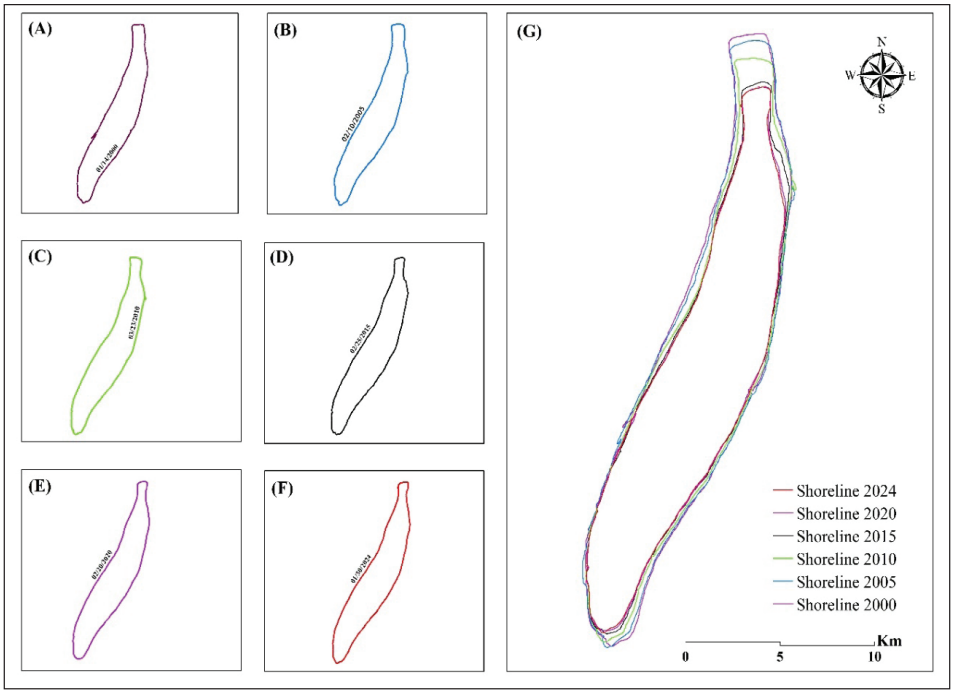

Figure 4: Extracted Shorelines from Different Years; (A) 2000, (B) 2005, (C) 2010, (D) 2015, (E) 2020, (F) 2024 and (G) Combined Shoreline Change from 2000 to 2024

Shoreline Change Rate

The distributions of EPR, WLR, and LRR along the transects, as depicted in figure 5, clearly demonstrate the enormous range of diversity in shoreline displacement and the predominance of erosion surrounding the island. Based on variations in shoreline modifications, the shoreline has been segmented into eight different zones (Fig. 5) by constructing and analyzing line diagrams from the statistical value of EPR, LRR, and WLR data. To assess the dependability of different zones generated from EPR, LRR and WLR statistics, a line diagram was also drawn using the NSM and SCE values (Fig. 6). The NSM followed a pattern similar to that of the EPR, WLR, and LRR, with the exception of SCE, which in certain areas exhibited a pattern opposite the others. While the gap between the NSM and SCE lines suggests erosion, their similar alignments suggest accretion (Al-Zubieri et al., 2020; Mahmud et al., 2020).

Statistics on coastline alteration for the various zones are compiled in Table 3. To represent the risk level throughout the study area, the eight zones were divided into five classes determined by average shoreline change rates: very high erosion (< -60 m/yr), high erosion (-60 to -30 m/yr), moderate erosion (-30 to -15 m/yr), low erosion (-15 to 0 m/yr), and low accretion (0 to 15 m/yr). Zone 1 (Z1), comprising transects 1–13, exhibits high erosion rates with mean EPR, LRR, and WLR values of -56.94 m/yr and -59.51 m/yr, respectively. These parameters show similar magnitudes and trends. Zone 2 (Z2), covering transects 14–160, is the only accretion-dominated zone, with mean EPR at 6.78 m/yr and LRR/WLR at 9.22 m/yr. Unlike Z1, values fluctuate on both sides of the x-axis. Zone 3 (Z3), encompassing transects 161–240, demonstrates moderate erosion, with mean EPR at -21.82 m/yr and LRR/WLR at -23.31 m/yr. Similar to Z1, the values align on the negative side. Zone 4 (Z4), made up of transects 241–316, represents an erosion-prone area with the lowest mean values of EPR (-12.76 m/yr) and LRR/WLR (-14.42 m/yr). Zone 5 (Z5), spanning transects 317–413, exhibits severe erosion, with mean EPR, LRR, and WLR values of -77.94 m/yr and -82.6 m/yr. Zone 6 (Z6), including transects 414–479, experiences moderate erosion, with mean EPR at -26.80 m/yr and LRR/WLR at -28.20 m/yr. Zone 7 (Z7), consisting of transects 480–666, is relatively stable, displaying minimal erosion, with mean EPR at -9.14 m/yr and LRR/WLR at -10.84 m/yr. Lastly, Zone 8 (Z8), covering transects 667–743, exhibits moderate erosion, with mean EPR at -23.62 m/yr and LRR/WLR at -25.48 m/yr.

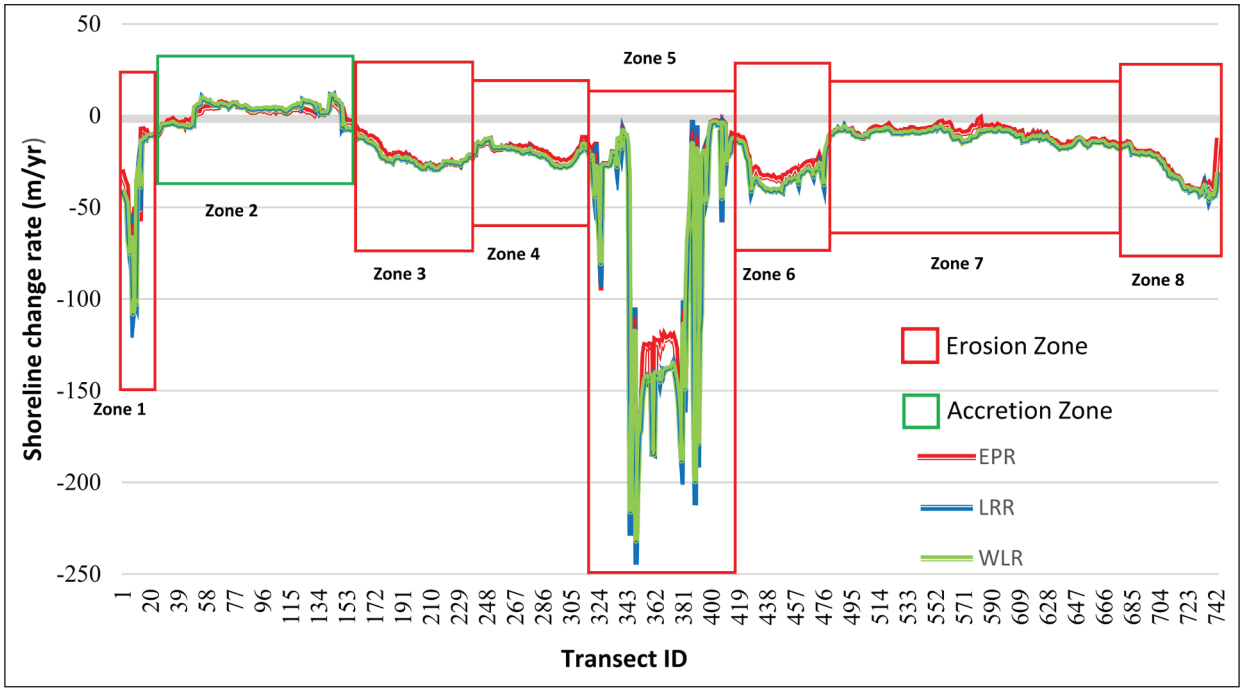

Figure 5: Based on the EPR, LRR, and WLR values around Manpura Island, the Shoreline was Segmented into Different Zones

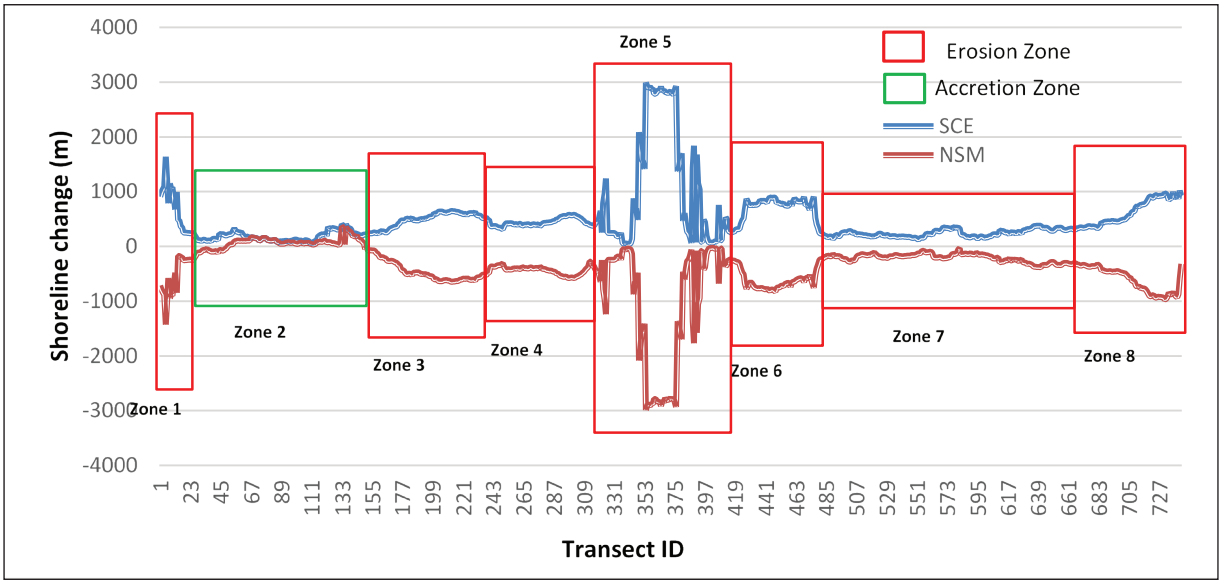

Figure 6: The Shorelines of the Island have been Segmented into Different Zones Based on NSM and SCE Values

The investigation revealed significant changes in the coastal region. The forecasted values for EPR, WLR, and LRR (Fig. 5), which coincide with NSM values (Fig. 6), indicate a minor accretion zone where sediments carried by estuarine water accumulate. From figure 6, it is certain that only one zone showed accretion, which has a small number of transects. The other 7 zones showed erosion. The peak erosion rate is 227.2 m/yr, whereas the peak accretion rate is 14.5 m/yr (Table 3). Manpura is unequivocally an island characterized by erosion. Several variables, including severe storms, alterations in bank composition, and anthropogenic activities, contribute to elevated erosion rates along shorelines (Mahmud et al., 2020; Islam et al., 2022).

Table 3: Summary of Shoreline Statistics Categorized by Zones for Manpura Island (Shoreline Changes are Represented in Meter for NSM and SCE and meter/year for EPR, LRR, and WLR)

Zone	Statistical Parameters	No. of Transects	Mean	Min.	Max.	Avg. R^2	Remarks
Z1	EPR	13	-56.94	-102.78	-31.15	0.44 0.38	High erosion
	LRR		-59.51	-107.87	-28.23		
	WLR		-59.51	-107.87	-28.23		
	NSM		-844.63	-1427.18	-478.37		
	SCE		1038.04	668.75	1636.8		
Z2	EPR	147	6.78	-11.02	14.51	0.86 0.83	Low accretion
	LRR		9.22	-13.69	19.44		
	WLR		9.22	-13.69	19.44		
	NSM		21.55	-153.88	358.17		
	SCE		194.34	43.24	480.28		
Z3	EPR	80	-21.82	-28.06	-8.52	0.66 0.58	Moderate erosion
	LRR		-23.31	-29.45	-11.98		
	WLR		-23.31	-29.45	-11.98		
	NSM		-502.86	-646.72	-196.42		
	SCE		515.71	251.55	646.72		
Z4	EPR	76	-12.76	-25.19	-7.14	0.90 0.83	Low erosion
	LRR		-14.42	-28.27	-7.65		
	WLR		-14.42	-28.27	-7.65		
	NSM		-432.44	-580.46	-279.69		
	SCE		437.51	315.06	580.46		
Z5	EPR	97	-77.94	-227.2	-23.04	0.30 0.41	Very high erosion
	LRR		-82.61	-231.72	-23.48		
	WLR		-82.61	-231.72	-23.48		
	NSM		-1070.54	-2990.46	-27.9		
	SCE		1089.89	33.97	2990.65		
Z6	EPR	66	-26.80	-35.88	-10.3	0.73 0.58	Moderate erosion
	LRR		-28.20	-41.71	-12.93		
	WLR		-28.20	-41.71	-12.93		
	NSM		-617.76	-826.74	-237.36		
	SCE		700.28	252.91	904.32		

	EPR		-9.14	-16.49	-1.59		
	LRR		-10.84	-18.04	-5.96	0.88	
Z7	WLR	187	-10.84	-18.04	-5.96	0.85	Low accretion
	NSM		-210.69	-380.57	-36.68		
	SCE		241.48	124.4	380.57		
	EPR		-23.62	-42.1	-13.73		
	LRR		-25.48	-45.94	-15.54	0.63	
Z8	WLR	77	-25.48	-45.94	-15.54	0.58	Moderate erosion
	NSM		-613.45	-970.08	-316.28		
	SCE		629.20	328.72	1018.16		

Shoreline Evaluation and Zonations

Figure 5 and Table 4 provide a detailed representation of shoreline dynamics, identifying specific regions at the island's extremities that are more vulnerable to erosion. Analyzing eight coastline zones during the study period, it was found that seven were predominantly affected by erosion. Among these, zone Z5 experienced very high erosion, zone Z1 had high erosion, zones Z3, Z6, and Z8 exhibited moderate erosion, while zones Z4 and Z7 experienced low erosion. In contrast, zone Z2 was classified as a modest accretion zone (Table 3).

Table 4: Mean Shoreline Change Rate of the Island from 2000 to 2004

Timeline	Mean LRR	Mean WLR	Mean EPR
Interval (2000-2005)	-5.94224	-5.9422398	-4.171
Interval (2005-2010)	-33.08737	-33.087371	-40.6171
Interval (2010-2015)	-18.34882	-18.348821	-14.4884
Interval (2015-2020)	-4.668081	-4.6680814	-4.31029
Interval (2020-2024)	-3.291858	-3.2918581	-1.20984
Interval (2000-2014)	-24.67	-25.67	-22.73
Overall mean shoreline change rate (m/yr)		-24.02	

The mean coastline erosion rate across all transects was approximately -24.02 m/year (Table 4). Most zones had low to moderate coefficients of determination (R^2), except for zones Z2 (0.86), Z4 (0.90), and Z7 (0.88), which had high R^2 values, indicating consistent erosion and accretion trends (Table 4). A high R^2 value (>0.80) signifies reliable predictions of shoreline change rates (Mahmud et al., 2020). Conversely, lower R^2 values in Zones Z1 (0.44) and Z5 (0.30), along with moderate R^2 values in zones Z3 (0.66), Z6 (0.73), and Z8 (0.63), suggest highly dynamic coastal processes with significant variations in erosion intensity.

Field surveys and local observations in zones Z1, Z2, Z5, and Z7 validated the shoreline changes determined by the DSAS method. Notably, Zone Z2 exhibited accretion following the construction of levees in 2020, resulting in limited land expansion. Residents reported ongoing land accretion in these areas at a rate of approximately 10–20 m/year. Additionally, field data aligned with DSAS findings, indicating that zones Z4 and Z7 have remained relatively stable with minimal erosion.

A comprehensive vulnerability assessment of the island's shoreline is presented in Figure 6, which features a color-coded grid map illustrating erosion

and accretion zones. This map highlights critical areas requiring immediate attention and provides insights into the relative stability of different coastline sections. Zones Z1 and Z5 are particularly susceptible to active erosion, emphasizing the urgent need for wave breaker structures, coastal protection measures, and other shoreline defense mechanisms (Al-Zubieri et al., 2020). In contrast, zones Z3, Z4, Z6, Z7, and Z8 exhibit moderate to low erosion susceptibility, while zone Z2 remains dominated by accretion.

The analysis underscores the highly dynamic nature of the shoreline, where areas of accretion can rapidly transition to erosion within short time frames. Notably, accretion-dominated processes are concentrated on the southwestern side of the island, whereas erosion-prone zones are primarily located near the river mouth and along the seaward-facing sections of the coastline (Fig. 7). The powerful wave action of the GBM (Ganges-Brahmaputra-Meghna) river system resulted in significantly greater erosion on the riverine side of the island than sediment accumulation. The coastal zone of the island underwent these changes, with the most significant changes occurring at marine heads in the northern tip and southeast areas. The shoreline in the north-eastern and southwest parts of the island underwent moderate to minor changes (Fig. 7). The geomorphology of these marine heads may have changed as a result of coastal processes like wave energy, longshore currents, and the influence of tides, but few consecutive erosional and accretional activities are occurring along the coast due to human intervention (Al-Zubieri et al., 2020, Islam et al., 2022).

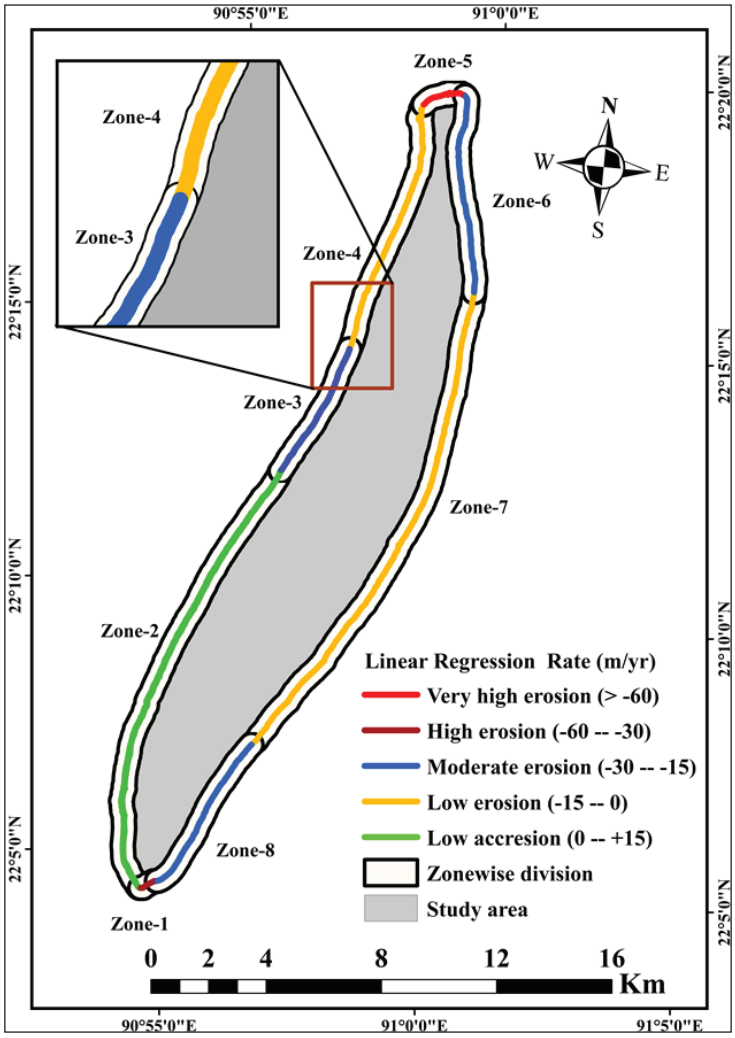

Figure 7: Shoreline Evolution Zone Map of the Manpura Island

CONCLUSIONS AND FUTURE IMPLICATIONS

Manpura, the dynamic coastal island of Bangladesh is highly vulnerable to natural disasters. To better understand and mitigate these impacts, this study analyzed shoreline evolution on Manpura Island over a 24-year period using GIS-based techniques and the Digital Shoreline Analysis System (DSAS). Landsat 5, 7, and 8 satellite images from the dry seasons were used to assess shoreline changes through the Shoreline Change Envelope (SCE), Net Shoreline Movement (NSM), and Linear Regression Rate (LRR) methods.

The analysis revealed severe shoreline erosion across Manpura Island. Of the 743 transects examined, 643 indicated significant erosion, while only 100 showed minor accretion. The mean rate of shoreline change was calculated as -24.02 m/year, with the northern coast experiencing the most rapid erosion at up to 77.94 m/year. Over the 24-year period, approximately 26.27 km² of land was lost, with erosion dominating over the minimal 2.56 km² of accretion observed. These results highlight the island's critical state of erosion, driven by natural forces such as sediment transport and tidal dynamics, compounded by human activities and the increasing impacts of climate change.

The DSAS tool proved to be highly effective for quantifying and visualizing shoreline change compared to manual digitization or simpler statistical approaches. Its ability to integrate multiple shoreline datasets, compute change metrics, and generate spatially explicit erosion rates makes it particularly suitable for long-term monitoring. Future applications of DSAS, combined with high-resolution satellite imagery (e.g., Sentinel-2 or PlanetScope), can further enhance the accuracy of global shoreline change assessments and support the development of adaptive coastal management strategies in vulnerable regions like Bangladesh.

CONFLICT OF INTEREST

The authors state that the research was conducted in the absence of any commercial or financial affiliations that could be construed as a potential conflict of interest.

DATA AVAILABILITY

The data presented in this study are available upon request from the corresponding author.

FUNDING

This research received no external funding.

ACKNOWLEDGEMENT

The authors are grateful to United States Geological Survey (USGS) for the data used for the research. The authors also extend their gratitude to the people of Manpura Island for their spontaneous participation in the questionnaire survey for validation of the research.

REFERENCES

Ahmed, A., Drake, F., Nawaz, R., Woulds, C., 2018. Where is the coast? Monitoring coastal land dynamics in Bangladesh: An integrated management approach using GIS and remote sensing techniques. Ocean & Coastal Management 151, 10–24.

Ahmed, A., Nawaz, R., Woulds, C., Drake, F., 2020. Influence of hydro-climatic factors on future coastal land susceptibility to erosion in Bangladesh: A geospatial modelling approach. Journal of Geovisualization and Spatial Analysis 4, 1–24.

Ahmed, I., Das, N., Debnath, J., Bhowmik, M., 2018. Erosion-induced channel migration and its impact on dwellers in the lower Gumti River, Tripura, India. Spatial Information Research 26, 537–549.

Ahmed, N., Howlader, N., Hoque, M. A.-A., Pradhan, B., 2021. Coastal erosion vulnerability assessment along the eastern coast of Bangladesh using geospatial techniques. Ocean & Coastal Management 199, 105408.

Akhter, F., Hoque, M. E., Xu, N., 2024. Geospatial analysis of shoreline and areal dynamics in the Ganges deltaic island of Bangladesh using the GIS-DSAS technique. Regional Studies in Marine Science 73, 103495. https://doi.org/10.1016/j.rsma.2024.103495

Ali, M. S., Haque, M. F., Rahman, S. M. M., Iqubal, K. F., Nazma, M., & Ahmed, A. (2013). Loss and gain of land of Manpura Island of Bhola District: An integrated approach using remote sensing and GIS. Dhaka University Journal of Biological Sciences, 22, 29–37. https://doi.org/10.3329/dujbs.v22i1.46271

Al-Zubieri, A. G., Ghandour, I. M., Bantan, R. A., Basaham, A. S., 2020. Shoreline evolution between Al Lith and Ras Mahāsin on the Red Sea coast, Saudi Arabia using GIS and DSAS techniques. Journal of the Indian Society of Remote Sensing 48(10), 1455–1470. https://doi.org/10.1007/s12524-020-01169-6

Banglapedia, 2023. Manpura Upazila. National Encyclopedia of Bangladesh. https://en.banglapedia.org/index.php/Manpura_Upazila

Banglapedia, 2024. Manpura Upazila. https://en.banglapedia.org/index.php/Manpura_Upazila

Begum, A., Billah, S. M., 2012. Predicted potentialities of soil resources of the Manpura Island for tomato. South Asian Journal of Agriculture 5, 187–191.

Bernzen, A., Jenkins, J. C., Braun, B., 2019. Climate change-induced migration in coastal Bangladesh? A critical assessment of migration drivers in rural households under economic and environmental stress. Geosciences 9, 51.

Bheeroo, R. A., Chandrasekar, N., Kaliraj, S., Magesh, N. S., 2016. Shoreline change rate and erosion risk assessment along the Trou Aux Biches–Mont Choisy beach on the northwest coast of Mauritius using GIS-DSAS technique. Environmental Earth Sciences 75, 1–12.

Bhowmik, M., Das, C., Ahmed, I., Debnath, J., 2018. Bank material characteristics and its impact on river bank erosion, West Tripura District, Tripura, North-East India. Current Science 115, 1571–1576.

Biswas, R. N., Islam, M. Nazrul, Islam, M. Nazrul, Mia, M. J., Jahan, M. N., Shaunak, M. F., Rahman, M. M., Islam, M. Y., 2022. Impacts of morphological change on coastal landscape dynamics in Monpura Island in the northern Bay of Bengal, Bangladesh. Regional Studies in Marine Science 53, 102403.

Boak, E. H., Turner, I. L., 2005. A review of coastal shoreline definition and detection. Journal of Coastal Research.

Chatterjee, S., Mistri, B., 2013. Impact of river bank erosion on human life: A case study in Shantipur Block, Nadia District, West Bengal. Population (Paris) 66, 7–17.

Chirala, U., Gurram, M. K., Kinthada, N. R., 2015. Mapping of soil erosion zones of Meghadrigedda catchment, Visakhapatnam, India for conservation—A geospatial approach. International Journal of Geosciences 6, 326–338.

Coca, O., Ricaurte-Villota, C., 2022. Regional patterns of coastal erosion and sedimentation derived from spatial autocorrelation analysis: Pacific and Colombian Caribbean. Coasts, 2, 125–151.

Debanshi, J., Mandal, S., 2014. Dynamicity of the river Ganga and bank-erosion-induced land loss in Manikchak Diara of Malda district of West Bengal, India: A RS and GIS-based study. International Journal of Applied Remote Sensing & GIS 3, 43–56.

Dukes, J. S., Mooney, H. A., 2004. Disruption of ecosystem processes in western North America by invasive species. Revista Chilena de Historia Natural 77, 411–437.

Dutta, M. K., Barman, S., Aggarwal, S. P., 2010. A study of erosion–deposition processes around Majuli Island, Assam. Earth Science India, 3.

Duvat, V. K. E., 2019. A global assessment of atoll-island planform changes over the past decades. Wiley Interdisciplinary Reviews: Climate Change 10, e557.

Feyisa, G. L., Meilby, H., Fensholt, R., Proud, S., 2014. Automated Water Extraction Index (AWEI): A new technique for surface water mapping using Landsat imagery. Remote Sensing of Environment.

Frazier, P. S., Page, K. J., 2000. Water body detection and delineation with Landsat TM data. Photogrammetric Engineering & Remote Sensing 66, 1461–1468.

Ghorai, D., Mahapatra, M., 2020. Extracting shoreline from satellite imagery for GIS analysis. Remote Sensing in Earth Systems Sciences 3, 13–22.

Gorle, G., Reddy, M. G., Kumar, A. A., 2024. Coastal erosion and engineering solutions along Visakhapatnam coastline, east coast of India. Ecological Engineering & Environmental Technology, 25.

Haque, M. A., Shishir, S., Mazumder, A., Iqbal, M., 2023. Change detection of Jamuna river and its impact on the local settlements. Physical Geography 44, 186–206.

Himmelstoss, E. A., Henderson, R. E., Kratzmann, M. G., Farris, A. S., 2018. Digital shoreline analysis system (DSAS) version 5.0 user guide (Open-File Report 2018–1179). U.S. Geological Survey. https://doi.org/10.3133/ofr20181179

Himmelstoss, E. A., Henderson, R. E., Kratzmann, M. G., Farris, A. S., 2021. Digital shoreline analysis system (DSAS) version 5.1 user guide (Open-File Report 2021–1091). U.S. Geological Survey.

Holman, R. A., Stanley, J., 2007. The history and technical capabilities of Argus. Coastal Engineering 54, 477–491.

Islam, M. A., Hasan, M., Peas, M. H., Naime, M. A., Gazi, M. Y., Rahman, M. M., 2016. Shoreline vulnerability assessment in an offshore island (Sandwip), Bangladesh—An appraisal of geospatial techniques. Dhaka University Journal of Earth and Environmental Sciences 5, 51–60.

Islam, M. K., Hasan, M., Rahman, M., Fayyaz, R., Chowdhury, M., Hamid, T., 2023. Shoreline dynamics assessment of Moheshkhali Island of Bangladesh using integrated GIS-DSAS techniques. The Dhaka University Journal of Earth and Environmental Sciences 11(1), 1–14.

Islam, M. N., van Amstel, A., Malak, M. A., Hossain, N. J., Quader, M. A., Akter, T., Islam, M. N., 2021. Climate change-induced natural hazard: Population displacement, settlement relocation, and livelihood change due to riverbank erosion in Bangladesh. In Bangladesh II: Climate Change—Impacts, Mitigation and Adaptation in Developing Countries (pp. 193–210).

Islam, M. S., Crawford, T. W., Shao, Y., 2023. Evaluation of predicted loss of different land use and land cover due to coastal erosion in Bangladesh. Frontiers in Environmental Science 11, 1144686.

Islam, M. S., Hossain, M. A., Lina, R. I., 2019. Forced migration as a livelihood adaptation in response to climate change: An empirical study on Central South exposed coast of Bangladesh. Social Change, 13.

Kannan, R., Kanungo, A., Murthy, M. V. R., 2016. Detection of shoreline changes, Visakhapatnam coast, Andhra Pradesh, from multi-temporal satellite images. Journal of Remote Sensing & GIS 5, 157.

Khan, M. H., 2012. River erosion and its socio-economic impact in Barpeta District with special reference to Mandia Development Block of Assam. International Journal of Engineering Sciences 1, 177–183.

Khan, N. I., Islam, A., 2003. Quantification of erosion patterns in the Brahmaputra–Jamuna River using geographical information system and remote sensing techniques. Hydrological Processes 17, 959–966.

Kumar, L., Eliot, I., Nunn, P. D., Stul, T., McLean, R., 2018. An indicative index of physical susceptibility of small islands to coastal erosion induced by climate change: An application to the Pacific islands. Geomatics, Natural Hazards and Risk 9, 691–702.

Liang, T. Y., Chang, C. H., Hsiao, S. C., Huang, W. P., Chang, T. Y., Guo, W. D., Chen, W. B., 2022. On-site investigations of coastal erosion and accretion for the northeast of Taiwan. Journal of Marine Science and Engineering 10(2), 282.

Mahmud, M. I., Mia, A. J., Islam, M. A., Peas, M. H., Farazi, A. H., Akhter, S. H., 2020. Assessing bank dynamics of the lower Meghna river in Bangladesh: An integrated GIS-DSAS approach. Arabian Journal of Geosciences 13(14). https://doi.org/10.1007/s12517-020-05514-4

McFeeters, S. K., 1996. The use of the normalized difference water index (NDWI) in the delineation of open water features. International Journal of Remote Sensing.

Mentaschi, L., Vousdoukas, M. I., Pekel, J. F., Voukouvalas, E., Feyen, L., 2018. Global long-term observations of coastal erosion and accretion. Scientific Reports 8, 1–11.

Nassar, K., Mahmod, W. E., Fath, H., Masria, A., Nadaoka, K., Negm, A., 2019. Shoreline change detection using DSAS technique: Case of North Sinai coast, Egypt. Marine Georesources & Geotechnology 37, 81–95.

Pereira, G. F., Gurugnanam, B., Goswami, S., Choudhury, S., 2022. Application of geospatial techniques to determine coastal erosion and accretion along the Ramanathapuram shore, Tamil Nadu, India. Journal of the Geological Society of India 98, 1261–1270.

Pimentel, D., Kounang, N., 1998. Ecology of soil erosion in ecosystems. Ecosystems, 1, 416–426.

Quang, D. N., Ngan, V. H., Tam, H. S., Viet, N. T., Tinh, N. X., Tanaka, H., 2021. Long-term shoreline evolution using DSAS technique: A case study of Quang Nam Province, Vietnam. Journal of Marine Science and Engineering 9(10), 1124.

Rahman, M. R., 2010. Impact of riverbank erosion hazard in the Jamuna floodplain areas in Bangladesh. Journal of Science Foundation 8, 55–65.

Ramalho, R. S., Quartau, R., Trenhaile, A. S., Mitchell, N. C., Woodroffe, C. D., Ávila, S. P., 2013. Coastal evolution on volcanic oceanic islands: A complex interplay between volcanism, erosion, sedimentation, sea-level change and biogenic production. Earth-Science Reviews 127, 140–170.

Saha, M., Sauda, S. S., Real, H. R. K., Mahmud, M., 2022. Estimation of annual rate and spatial distribution of soil erosion in the Jamuna Basin using RUSLE model: A geospatial approach. Environmental Challenges 8, 100524.

The Daily Star, (2017, May 16). Save Manpura from river erosions. The Daily Star.

Thieler, E. R., Himmelstoss, E. A., Zichichi, J., Ergul, A., 2009. The digital shoreline analysis system (DSAS) version 4.0—An ArcGIS extension for calculating shoreline change (Open-File Report 2008–1278). U.S. Geological Survey. https://doi.org/10.3133/ofr20081278

Thomas, A., Benjamin, L., 2018. Policies and mechanisms to address climate-induced migration and displacement in Pacific and Caribbean small island developing states. International Journal of Climate Change Strategies and Management 10, 86–104.

Turner, I. L., Harley, M. D., Drummond, C., 2016. Coastal imaging and UAV–Structure-from-Motion for beach monitoring. Coastal Engineering.

United Nations, 2015. Transforming our world: The 2030 Agenda for Sustainable Development. https://sdgs.un.org/2030agenda

Vallarino-Castillo, R., Negro-Valdecantos, V., del Campo, J. M., 2024. A systematic review of oceanic–atmospheric variations and coastal erosion in continental Latin America: Historical trends, future projections, and management challenges. Journal of Marine Science and Engineering 12, 1077.

Xu, H., 2006. Modification of NDWI to enhance open water features: MNDWI. Photogrammetric Engineering & Remote Sensing.